

ACCURATE HELLMANN-FEYNMAN FORCE METHOD FOR THE STUDY OF THE
FIRST AND SECOND DERIVATIVES OF POTENTIAL ENERGY HYPERSURFACE

H. Nakatsuji and K. Kanda

Department of Hydrocarbon Chemistry
Faculty of Engineering
Kyoto University, Kyoto, Japan

1. INTRODUCTION

Hellmann-Feynman (H-F) theorem gives an intuitive expression of the force based on an electrostatic interaction between the electron density and nuclei.¹ This simplicity is very valuable in studying complex chemical phenomena such as molecular geometry, chemical reaction and molecular vibration.² A past defect of this approach was that the calculation of a wavefunction which satisfies the H-F theorem was believed to be difficult.³

However, we recently found a promising method of calculating a reliable H-F force.⁴⁻⁷ Here, we briefly review the method starting from the underlying theorem and examine the accuracy of the calculated H-F force. We then show some recent applications of the method to geometry optimizations of the molecules in ground and excited states and of the transition state of a chemical reaction. It has also been applied to the analysis of chemical reaction paths.⁸

Further, when we use the H-F theorem, an analytic expression of the second derivative of energy becomes much simpler and more perspective than a straightforward second derivative of the energy.^{7,9} We report calculations of force constants (both positive and negative) by this method and explain the electronic origins of the second derivatives.

2. THEOREM

A force acting on nucleus A, \underline{F}_A is written as

$$\begin{aligned} \underline{F}_A &= - \langle \Psi | \partial H / \partial \underline{R}_A | \Psi \rangle - \langle \partial \Psi / \partial \underline{R}_A | H | \Psi \rangle - \langle \Psi | H | \partial \Psi / \partial \underline{R}_A \rangle \\ &= - \langle \Psi | \partial H / \partial \underline{R}_A | \Psi \rangle - \sum_r \underline{\Delta}_r \partial \underline{x}_r / \partial \underline{R}_A \end{aligned} \quad (1)$$

where the first term is the H-F force and the rest is an error term which vanishes identically for a correct wavefunction. It is expressed as a sum of the AO error $\underline{\Delta}$ associated with each basis χ_r . (In Eq. (1), \underline{R}_A is a nuclear coordinate and \underline{x}_r the center of a basis χ_r .) It is shown that the AO error is expressed as

$$\underline{\Delta}_r = 2 \sum_i c_{ri} \text{ (SCF requirement projected on } |r'\rangle \text{)} \quad (2)$$

where c_{ri} is a mixing coefficient of the basis χ_r in an orbital ϕ_i , and r' is a derivative $\partial \chi_r / \partial \underline{x}_r$ of the basis $r = \chi_r$. Eq. (2) proves the following theorem:

A sufficient condition for a general SCF wavefunction to satisfy the Hellmann-Feynman theorem is that the basis set includes the derivative r' for any basis r . The basis set $\{r, r', r'', \dots\}$ is such a basis. If the basis is recurrent in the sense $r = r^{(n)}$, then the number of elements can be finite.

This theorem is valid for general SCF theories including closed-shell Hartree-Fock, UHF, RHF for open-shell and excited states, general MC-SCF, and some types of GVB theory. Note that if only the force acting on a nucleus A, \underline{F}_A , is concerned, the derivative r' may be added only to those bases whose centers are on the nucleus A (see Eq. (1)).

3. A NEW FORCE METHOD

The above theorem gives a basis for a systematic method of improving a wavefunction so that it satisfies the Hellmann-Feynman theorem. As a first stage of such an approach, we have considered an approximation in which only the first derivative AO's $\{r'\}$ are added to the "parent" AO's $\{r\}$. (The set $\{r, r'\}$ is called a "family".) Then, all of the AO errors of the parent AO's vanish identically as Eq. (2) shows, but the AO errors of the added derivative AO's remain. However, if the parent basis set is already a good basis, the mixing coefficient $c_{r'i}$ of the added derivative AO's r' should be small, so that from Eq. (2) the AO error of the added AO r' , $\underline{\Delta}_{r'}$, may be neglected. This approximation has been confirmed to be very good: test calculations were performed for the closed-shell Hartree-Fock method,^{4,6} open-shell RHF⁵ and UHF methods, and MC-SCF method.⁵ Further, it was also shown that other properties, such as dipole moment, quadrupole moment, etc., are improved at the same time.⁶

Table 1. AO error, Hellmann-Feynman force and energy gradient of CO (a.u.).^{a,b}

	Force on Carbon		Force on Oxygen	
	Parent [3s2p]	Family [3s2p] plus first derivatives	Parent [3s2p]	Family [3s2p] plus first derivatives
AO error				
s1	0.4943	0.0062	-0.7986	-0.0079
s2	-0.0932	0.0052	0.0167	0.0
s3	0.0012	0.0002	-0.0096	-0.0008
p1 σ	0.3816	0.0117	-0.7835	-0.0248
p2 σ	0.0023	0.0003	-0.0036	-0.0002
p1 π	0.2574	0.0104	-0.6379	-0.0102
p2 π	-0.0001	0.0002	-0.0005	-0.0014
Total error	1.3007	0.0446	-2.8553	-0.0565
H-F force	-3.1998	-1.7094	4.7543	1.7213
Energy gradient	-1.8990	-1.6648	1.8990	1.6648

^aThe CO length is 0.8636 Å (experimental equilibrium length, 1.1283 Å). The CO is on the σ axis in the direction from C to O. The [3s2p] set is due to Dunning and Hay.⁹

^bSCF energy is -112.3278 a.u. for the parent set and -112.4480 a.u. for the family set.

4. APPLICATION OF THE NEW FORCE METHOD

Table 1 shows the AO error, H-F force, and energy gradient of CO obtained from the parent and family sets of the [3s2p] set.¹⁰ By the addition of the first derivative AO's, the error term decreases dramatically. With the family set, the H-F force agrees well with the direct energy gradient, showing that the H-F theorem is essentially satisfied. The energy lowering due to an addition of the first derivative AO's (a kind of polarization function) is 0.1202 a.u.

Figure 1 shows plots of the transverse forces acting on the proton of H₂O, calculated by several methods, against the HOH angle. When we use the family set, the curves for the H-F force and the energy gradient almost superpose each other; the H-F theorem is satisfied over a wide range of valence angle. Further, by the addition of the first derivative AO's, the calculated equilibrium angle changes from 112.5° to 107.0° and becomes closer to the experimental value, 104.5°.

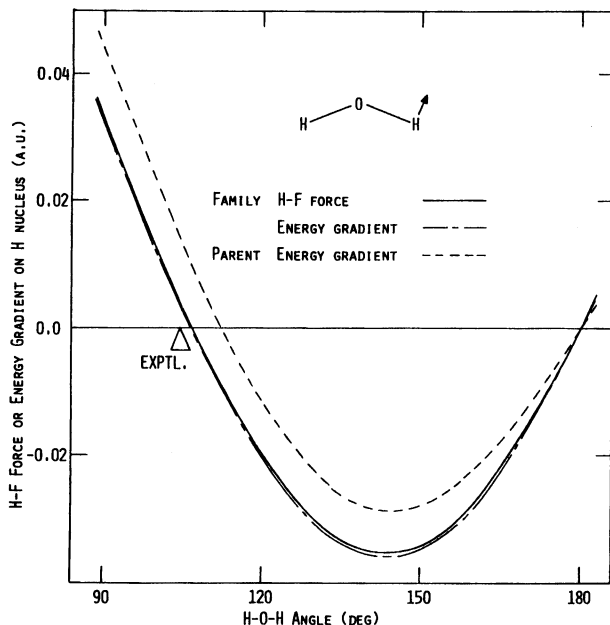


Fig. 1. Hellmann-Feynman force and energy gradient for the transverse force acting on the proton of H_2O vs the bond angle. The basis sets are the parent and family sets of the $[3s2p/2s]$ set.¹⁰

Table 2 shows the bond lengths and force constants of several diatomic molecules. When the family sets are used, the calculated values are essentially the same independent of the forces used. In further examination, the H-F force method tends to give a bond length a bit longer ($\sim 0.01 \text{ \AA}$) than the energy gradient values. Comparing the results of the parent and family sets, we see that the force constants are improved considerably by the addition of the first derivative AO's.

Table 3 shows the geometries of the ground state, triplet excited state, and ionized state of HNO determined by the present H-F force method. We have used closed and open-shell RHF method. Since the $\pi \rightarrow \pi^*$ transition reduces the electron density from the π bonding region of the N-O bond, the N-O length increases by this transition. The same is true for the ionization from the π MO. Since both $\pi \rightarrow \pi^*$ transition and the ionization from π MO do not cause much change in the electron density on the σ plane, the changes in the N-H length and the HNO angle are relatively small.

Table 2. Bond lengths and force constants of diatomic molecules AB.^a

Molecule	Property	Parent: [3s2p/2s] energy gradient	Family: [3s2p/2s] plus first derivatives energy gradient	H-F force on A	H-F force on B	Exptl.
LiH	bond length (Å)	1.632	1.604	1.599	1.608	1.596
	force constant (mdyn/Å)	1.203	1.112	1.092	1.112	1.025
BH	bond length (Å)	1.243	1.229	1.235	1.232	1.232
	force constant (mdyn/Å)	3.308	3.196	3.149	3.198	3.046
CO	bond length (Å)	1.138	1.114	1.124	1.127	1.128
	force constant (mdyn/Å)	22.15	20.05	20.47	20.32	19.02
N ₂	bond length (Å)	1.100	1.074	1.084	1.084	1.098
	force constant (mdyn/Å)	28.15	25.25	25.50	25.50	22.95
LiF	bond length (Å)	1.606	1.566	1.570	1.583	1.564
	force constant (mdyn/Å)	3.239	2.731	2.717	2.775	2.502

^aThe force constants are calculated at the experimental equilibrium geometry.

Table 3. Geometries of the ground state, triplet excited state, and ionized state of HNO determined by the Hellmann-Feynman force.^a

State		R(N-O) Å	R(N-H) Å	HNO deg
Ground	Force-optimized	1.193	1.029	108.8
	Exptl.	1.212	1.063	108.6
3($\pi \rightarrow \pi^*$)	Excited Force-optimized	1.538	1.015	101.5
2($\pi \rightarrow \infty$)	Ionized Force-optimized	1.297	1.011	110.9

^aThe family set of the 4-31G set is used.

5. ANALYTIC SECOND DERIVATIVE OF POTENTIAL ENERGY

When the Hellmann-Feynman theorem is satisfied for the first derivative of energy, the analytic expression of the second derivative becomes much simpler than the straightforward second derivative of the energy. Further, the intuitive physical meaning of the H-F force is extended to the second derivative. Though these merits have been noted by several authors,⁹ it was difficult to realize them, except for some simple systems, because of a lack of a practical method to calculate a wavefunction which satisfies the H-F theorem. However, the present approach has removed this obstacle.

A straightforward second derivative of the Hartree-Fock energy gives an expression

$$\begin{aligned}
 \frac{\partial^2 E}{\partial X_A \partial Y_B} = & \sum_{r,s} P_{rs} \frac{\partial^2 H_{rs}}{\partial X_A \partial Y_B} + \sum_{r,s} \frac{\partial P_{rs}}{\partial Y_B} \frac{\partial H_{rs}}{\partial X_A} + \frac{\partial^2 V_{nuc}}{\partial X_A \partial Y_B} \\
 & - \sum_{r,s} D_{rs} \frac{\partial^2 S_{rs}}{\partial X_A \partial Y_B} - \sum_{r,s} \frac{\partial D_{rs}}{\partial Y_B} \frac{\partial S_{rs}}{\partial X_A} \\
 & + \frac{1}{2} \sum_{rstu} P_{rs} P_{tu} \left[\frac{\partial^2}{\partial X_A \partial Y_B} (rt || su) \right] \\
 & + \sum_{rstu} \frac{\partial P_{rs}}{\partial Y_B} P_{tu} \left[\frac{\partial}{\partial X_A} (rt || su) \right]
 \end{aligned} \tag{3}$$

where H_{rs} , S_{rs} , and P_{rs} are the core-Hamiltonian matrix overlap matrix, and bond order density matrix, respectively and

$$D_{rs} = \sum_i^{\text{occ}} \epsilon_i^c r_i^c s_i$$

with ϵ_i the orbital energy. $(rt||su)$ is an appropriate sum of the Coulomb and exchange repulsion integrals¹¹ and V_{nuc} is the nuclear repulsion energy. On the other hand, when the H-F theorem is satisfied for the first derivative, only the parts of the first three terms of Eq. (3) remain. Most of the complex terms drop out, and we obtain

$$\begin{aligned} \frac{\partial^2 E}{\partial X_A \partial Y_B} &= \frac{\partial^2 V_{\text{nuc}}}{\partial X_A \partial Y_B} + \sum_{r,s} P_{rs} \delta_{AB} Z_A \langle r | \frac{\partial}{\partial Y_A} \left(\frac{x_A}{r_A^3} \right) | s \rangle \\ &+ \sum_{r,s} P_{rs} Z_A \left(\langle \frac{\partial r}{\partial Y_B} \left| \frac{x_A}{r_A^3} \right| s \rangle + \langle r | \frac{x_A}{r_A^3} \left| \frac{\partial s}{\partial Y_B} \right. \right) \\ &+ \sum_{r,s} \frac{\partial P_{rs}}{\partial Y_B} Z_A \langle r | \frac{x_A}{r_A^3} | s \rangle \end{aligned} \quad (4)$$

where

$$\frac{\partial}{\partial Y_A} \left(\frac{x_A}{r_A^3} \right) = \begin{cases} (r_A^2 - 3x_A^2)/r_A^5 + \frac{4}{3}\pi\delta(A) & X_A = Y_A \\ -3x_A y_A / r_A^5 & X_A \neq Y_A \end{cases} \quad (5)$$

Thus equation is much simpler to calculate than Eq. (3) and, furthermore, a simple physical meaning is associated with each term as follows. The first two terms of Eq. (4) show a change in the H-F force when only nucleus A is moved while the electron density surrounding it remains unaltered. They consist of an electric field gradient at nucleus A and a contribution from the density at the nucleus (Fermi term). The third term includes the derivative of the basis AO's and represents the H-F force on A due to the displaced AO's of atom B with keeping the AO coefficients unaltered. Then, the sum of the first three terms shows a net effect when the nucleus and the AO's associated with it are moved simultaneously without changing their AO coefficients (complete following²). The last term represents the effect of reorganization of the electron density matrix due to the nuclear motion, $\partial P_{rs}/\partial Y_B$. It arises from the two sources since it is given by a sum of the two terms

$$\begin{aligned} \frac{\partial P_{rs}}{\partial Y_B} &= \sum_{i,j}^{\text{occ}} c_{ri} c_{sj} S_{ij}^{(1)} \\ &+ \sum_i^{\text{occ}} \sum_a^{\text{unocc}} u_{ai}^{(1)} (c_{ri} c_{sa} + c_{ra} c_{si}) \end{aligned} \quad (6)$$

where $S_{ij}^{(1)}$ is a derivative of the overlap $\langle \phi_i | \phi_j \rangle$ and $u_{a1}^{(1)}$ is a mixing coefficient between occupied and unoccupied MO's. The first term is the renormalization term which arises in order to keep the total wavefunction normalized during the vibration and the second term represents the relaxation of molecular charge distribution during the vibration through a mixing between occupied and unoccupied orbitals.

The role of the reorganization term during a nuclear rearrangement process is generally very important. The renormalization term usually gives a positive contribution to the force constant and is one of the important origins of the electron-cloud incomplete following, which is a density origin of a stable geometry.² On the other hand, the relaxation term usually gives a negative contribution to the force constant and works to lower the barrier. It is a origin of the electron-cloud preceding, which is a density origin of many nuclear rearrangement processes.² The role of the relaxation term during the course of a chemical reaction is of special interest.

6. CALCULATION OF THE SECOND DERIVATIVES OF STABLE MOLECULE AND TRANSITION STATE

The preceding formula for the second derivatives has been applied to the studies of the force constants of several di- and polyatomic molecules.^{7,8} Here, we show the results for CO and CH_5^- as prototypes of stable molecules and transition states. The later is the transition state of the reaction, $\text{CH}_4 + \text{H}^- \rightarrow \text{H}^- + \text{CH}_4$, which is a model of $\text{S}_{\text{N}}2$ reaction. We have used the family set of the 4-31G set, so that the H-F theorem is essentially satisfied for the first derivatives as shown in the previous section.

Table 4 shows the analysis of the second derivatives. The force constant of CO was expressed in two different ways, $-\partial F_{\text{C}}/\partial X_{\text{C}}$ and $\partial F_{\text{O}}/\partial X_{\text{O}}$. It is a sum of large cancelling contributions. The nuclear term is positive. The Fermi term and the displaced AO term are very large because of the large inner-shell contribution, but they are cancelling. The sum of the second to fourth terms represents the effect of the AO density completely following the nuclear motion. The sum of the nuclear and completely following terms is negative for CO. In the next three rows the reorganization terms are given. In Figure 2, we have given the contour map of the density differential

$$-\sum_{r,s} \frac{\partial P_{rs}}{\partial R_{AB}} \chi_r(\underline{r}) \chi_s(\underline{r})$$

It shows the change in density when the bond distance is shortened. For stretching mode the renormalization term seems always to be positive (Table 4). When two atoms A and B come closer, the overlaps between the AO's become larger. Therefore, in order to keep

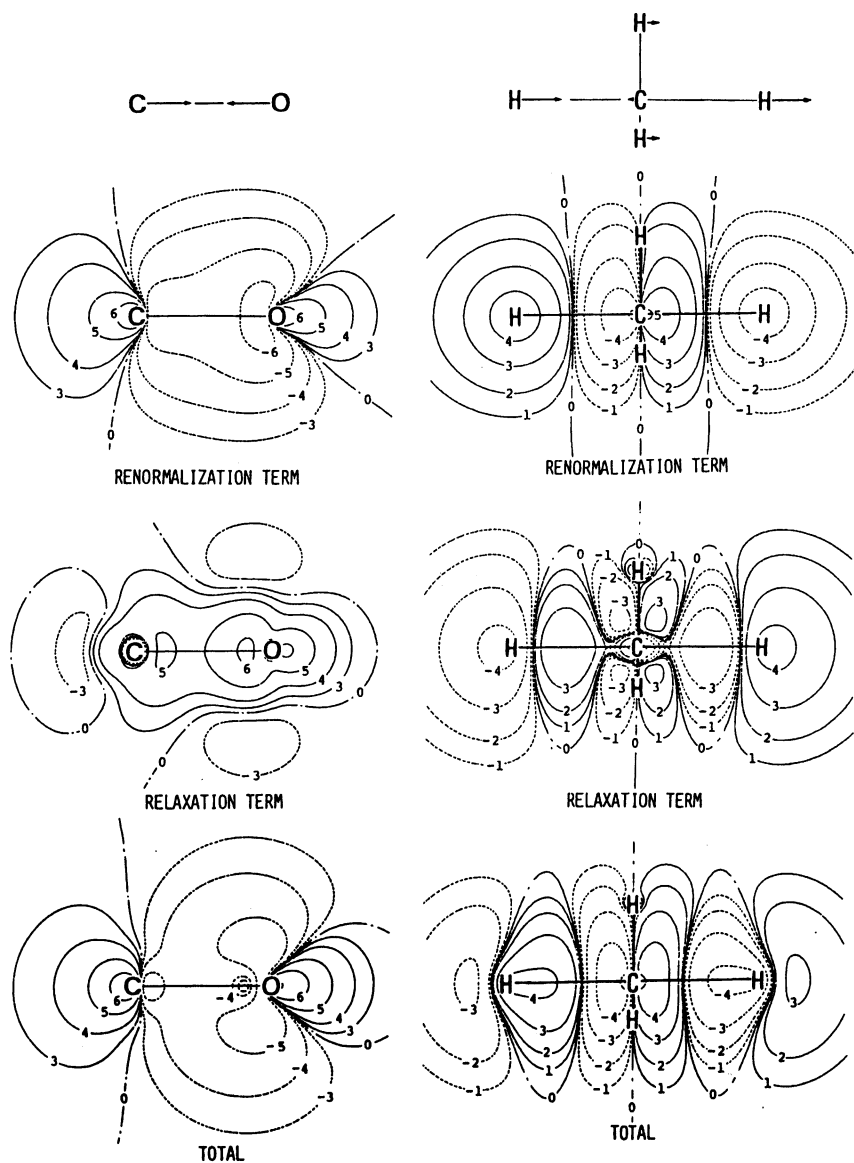


Figure 2. Contour map of the density differential $\sum \partial P_{rs} / \partial Q \times \chi_r(r) \chi_s(r)$ for CO and for the normal mode $Q_2(A_2^g)$ of CH_4 . From the top to the bottom, a sketch of the normal mode, the renormalization term, the relaxation term, and the sum of them are shown. The real lines correspond to an increase in density, and the broken lines correspond to a decrease, with the contour values of 0, ± 1 , ± 2 , ± 3 , ± 4 , ± 5 , and ± 6 corresponding to 0.0, ± 0.001 , ± 0.003 , ± 0.01 , ± 0.03 , ± 0.1 , and ± 0.3 a.u., respectively.

Table 4. Force constants of CO and CH₅ and their analyses (a.u.)

	CO ^a		CH ₅ ^b	
	$-\frac{\partial F_C}{\partial x_C}$	$\frac{\partial F_O}{\partial x_O}$	$\frac{\partial F}{\partial Q_1}(A'_1)$	$\frac{\partial F}{\partial Q_2}(A''_2)$
Nuclear term	9.906	9.906	0.440	0.142
$Z_A \int P_{rs} \langle r \frac{3x_A^2 - r_A^2}{r_A^5} s \rangle$	-16.522	-14.454	-0.412	-0.089
$Z_A \int P_{rs} \langle r -\frac{4}{3}\pi\delta(A) s \rangle$	3032.572	9899.184	1.371	79.873
$Z_A \int P_{rs} \langle r \frac{x_A}{r_A^3} s \rangle$	-3027.701	-9897.233	-1.337	-79.888
Total	-1.744	-2.596	0.062	0.038
Renormalization term	4.061	5.697	0.036	0.181
Relaxation term	-1.002	-1.785	-0.043	-0.329
Total	3.059	3.911	-0.007	-0.148
Grand total	1.315	1.315	0.055	-0.110
Experimental value	1.222	1.222		

^aCalculated for CO at the experimental geometry ($R_{CO}=1.1283$ Å) and for CH₅ at the transition state geometry determined by the present method (see text).

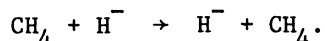
^bThe normal mode Q_1 is the totally symmetric C-H_a stretching mode and Q_2 is the so-called reaction coordinate. See figures in the text.

the total density normalized, the electron density should flow out of the A-B region as shown at the upper map of Figure 2. When two atoms A and B go apart, the reverse flow of electron density should occur. Thus, the density reorganization due to the renormalization term corresponds to the electron-cloud incomplete following² and gives a positive contribution to the force constant. On the other hand, in the relaxation term, the density increases in the bond region as the two atoms come closer. This behavior is the electron-cloud preceding² and works to stabilize the system. Then, the relaxation term gives negative contribution to the force constant as seen in Table 4. At the bottom of Figure 2, the total reorganization density is shown. It reflects mainly the renormalization term and then the net effect

of reorganization term gives positive contribution to the force constant.

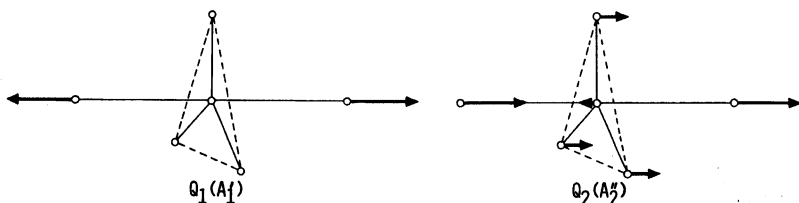
The calculated force constant of CO is 1.315 a.u. It is 7.6% larger than the experimental value. This is a trend of the Hartree-Fock results and an inclusion of electron correlation will reduce the difference. Though different analyses were obtained from $-\partial F_C/\partial X_C$ and $\partial F_0/\partial X_0$, the final results are the same because the H-F theorem is essentially satisfied for the first derivative.

We next show the results for the transition state CH_5^\ddagger of the reaction,



In the first stage, the geometry of the transition state was determined by the present force method. It was calculated to belong to the D_{3h} symmetry with $\text{C-H}_a = 1.700 \text{ \AA}$ and $\text{C-H}_e = 1.063 \text{ \AA}$ where H_a and H_e denote axial and equatorial hydrogens, respectively. This may be compared with the results of Dedieu and Veillard,¹² $\text{C-H}_a = 1.737 \text{ \AA}$ and $\text{C-H}_e = 1.062 \text{ \AA}$, and of Leforestier,¹³ $\text{C-H}_a = 1.70 \text{ \AA}$ and $\text{C-H}_e = 1.07 \text{ \AA}$.

The normal modes of the transition state CH_5^\ddagger are determined by diagonalizing the Hessian matrix. They consist of the twelve modes; the two A_1' , two A_2'' , three E' , and one E'' symmetry modes. Among these, one normal mode has negative force constant and all others have positive ones. In Table 4, we have shown only the two normal modes of the A_1' and A_2'' symmetries, which may be illustrated as



$Q_1(A_1')$ is the totally symmetric vibration of the axial C-H_a bonds. $Q_2(A_2'')$ is the so-called reaction coordinate involving Walden inversion and has negative force constant near the transition state.

In Table 4, we gave the second derivatives and their analyses. In comparison with CO, the Fermi and displaced AO terms are small because of a large contribution of the coordinates of hydrogens in the normal mode. This is especially so for the Q_1 mode in which carbon does not move during the mode. For CH_5^\ddagger , the sum of the nuclear term and the completely following term is positive in con-

trast to CO. From our experience, this seems to be common to the hydride molecules. A remarkable feature of the reaction coordinate Q_2 is that it has a large negative relaxation term. Because of this contribution, the force constant of the Q_2 mode is negative. At this geometry (transition state) the potential surface of CH_5 is maximum along the Q_2 coordinate and minimum for all others. For the coordinate Q_1 , the force constant is positive, though the reorganization term gives a small negative contribution.

An interesting behavior of electron density along the reaction coordinate is seen from the density differential map shown in the right-hand side of Figure 2. Referring to the relaxation term, we see a typical pattern of the electron-cloud preceding: the density reorganizes itself so as to precede the nuclear motion along the Q_2 coordinate. It occurs in all the regions near the moving nuclei, C, H_a , and H_e . In the renormalization term, however, the density near the C and H_e shows a pattern of the electron-cloud incomplete following. Near the H_a , the renormalization term also exhibits the electron-cloud preceding. In the total sum, the relaxation term surpasses the renormalization term and a beautiful pattern of the electron-cloud preceding is seen. As shown in Table 4, this is an origin of the negative force constant of the reaction coordinate Q_2 .

7. CONCLUSION

Here, we have viewed a possibility of an accurate Hellmann-Feynman force approach for the studies of the first and second derivatives of a potential energy hypersurface. Theoretical and physical simplicity of the underlying concept and the reliability of the calculated results would help us to further understand chemical phenomena and to construct a predictive model with a quantum-chemical intuition.

Now that the first obstacle along this approach has been removed, the next step would be (1) to develop a method which fully utilizes the structures of the theory for rapid computations of the desired wavefunction and (2) to apply the present approach to a wider field of chemistry to get a deeper understanding of the phenomena with intuitive concept and quantitative accuracy.

REFERENCES

1. B.M. Deb, ed. "The Force Concept in Chemistry", Van Nostrand Reinhold, New York, 1981.
2. For example, H. Nakatsuji and T. Koga, Force Models for Molecular Geometry, chapter 3 of reference 1.
3. For example, P. Pulay, Calculation of Forces by Non-Hellmann-Feynman Methods, chapter 9 of reference 1.

4. H. Nakatsuji, K. Kanda, and T. Yonezawa, Force in SCF Theories, Chem.Phys. Letters 75, 340 (1980).
5. H. Nakatsuji, T. Hayakawa, and M. Hada, Force in SCF Theories. MC-SCF and open-shell RHF theories, Chem.Phys. Letters 80, 94 (1981).
6. H. Nakatsuji, K. Kanda, M. Hada, and T. Yonezawa, Force in SCF Theories. Test of the New Method. J.Chem.Phys., in press.
7. H. Nakatsuji, K. Kanda, and T. Yonezawa, Force in SCF Theories. Second Derivative of Potential Energy, J.Chem.Phys., in press.
8. H. Nakatsuji, M. Hada, and K. Kanda, Force in SCF Theories. First and Second Derivatives of the Potential Energies of Chemical Reaction Systems, Int.J. Quantum Chem., to be published.
9. For example, J. Goodisman, Calculation and Interpretation of Force Constants, chapter 5 of reference 1.
10. T.H. Dunning, Jr. and P.J. Hay, Gaussian Basis Sets for Molecular Calculations, in: "Methods of Electronic Structure Theory," H.F. Schaefer III, ed., Plenum, New York, 1977.
11. J.A. Pople, R. Krishnan, H.B. Schlegel, and J.S. Binkley, Derivative Studies in Hartree-Fock and Møller-Plesset Theories, Int.J. Quantum Chem.Symp. 13, 225 (1979).
12. A. Dedieu and A. Veillard, A Comparative Study of Some S_N2 Reactions through ab initio Calculations, J.Am.Chem.Soc. 94, 6730 (1972).
13. C. Leforestier, Classical trajectories using the full ab initio potential energy surface $H^- + CH_4 \rightarrow CH_4 + H^-$, J.Chem.Phys. 68, 4406 (1978).